Brief Communications

BDNF Signaling during Learning Is Regionally Differentiated within Hippocampus

Lulu Y. Chen,[1] Christopher S. Rex,[1] Danielle T. Pham,[1] Gary Lynch,[1,2] and Christine M. Gall[1,3]

Departments of [1]Anatomy & Neurobiology, [2]Psychiatry & Human Behavior, and [3]Neurobiology & Behavior, University of California, Irvine, Irvine, California 92697

Learning-induced neurotrophic signaling at synapses is widely held to be critical for neuronal viability in adult brain. A previous study provided evidence that unsupervised learning of a novel environment is accompanied by activation of the TrkB receptor for brain-derived neurotrophic factor (BDNF) in hippocampal field CA1b of adult rats. Here we report that this effect is regionally differentiated, in accord with "engram" type memory encoding. A 30 min exposure to a novel, complex environment caused a marked, NMDA receptor-dependent increase in postsynaptic densities associated with activated (phosphorylated) Trk receptors in rostral hippocampus. Increases were pronounced in field CA3a, moderate in the dentate gyrus, and absent in field CA1a. Synapses with Trk activation were significantly larger than their neighbors. Surprisingly, unsupervised learning had no effect on Trk phosphorylation in more temporal sections of hippocampus. It thus appears that commonplace forms of learning interact with regional predispositions to produce spatially differentiated effects on BDNF signaling.

Introduction

Identification of discrete brain sites associated with the encoding of particular types of memory has been a central theme in neurobiological studies of learning since the "engram" concept was first advanced early in the last century (Schacter, 1982). While helping to organize work on the storage and retrieval of information, the engram concept also has fundamental implications for work on neurotrophic signaling in brain. A substantial literature has grown up around the broad idea that learning, acting through neurotrophic systems, promotes neuronal viability and thus slows the effects of aging (Valenzuela et al., 2007; Tapia-Arancibia et al., 2008). If so, then it follows from the engram hypothesis that a given form of learning will trigger growth chemistries in discrete portions of the cortical telencephalon; widespread activation would, by the same argument, require diverse forms of experience. The present studies tested the first of these propositions.

Brain-derived neurotrophic factor (BDNF), which is synthesized in an activity-dependent manner by central neurons (Isackson et al., 1991; Castrén et al., 1998; Greenberg et al., 2009), enhances neuronal growth and survival in a variety of experimental circumstances (Chao, 2003; Kalb, 2005). Recent work established that the learning-related theta pattern of afferent activity causes rapid activation (phosphorylation) of BDNF's TrkB receptor at synapses in apical field CA1 of adult hippocampal slices (Chen et al., 2010). The effect depended upon the presence of endogenous extracellular BDNF, presumably released during stimulation, and NMDA receptor-driven engagement of Src family kinases (Chen et al., 2010; Huang and McNamara, 2010).

Theta was considerably more effective than other stimulation regimens in the slice studies, suggesting that synaptic BDNF signaling is, as generally assumed, closely related to learning (Minichiello, 2009). Tests of this idea proved positive: A 30 min session of unsupervised learning in a complex environment caused a robust increase in the number of synapses associated with dense concentrations of phosphorylated TrkB in the same CA1 field evaluated in the slice experiments (Chen et al., 2010). Here we describe results from studies comparing the magnitude of learning-related synaptic Trk activation in the primary subfields of hippocampus (dentate gyrus, CA3, CA1), and at different points along the structure's septotemporal axis. The results demonstrate striking regional differences in the neurotrophic response of hippocampus to a brief learning episode.

Materials and Methods

All animal procedures were conducted according to the National Institutes of Health *Guide for the Care and Use of Laboratory Animals* and protocols approved by the Institutional Animal Care and Use Committee of the University of California at Irvine, including efforts to minimize suffering and numbers of animals used.

Unsupervised learning paradigm. Procedures were slightly modified from published work (Fedulov et al., 2007; Chen et al., 2010). The unsupervised learning (USL) behavioral box (46 × 91 × 41 cm for length, width, and height, respectively) included a large open field and a closed-top dark compartment with a small entrance. Six-week-old male Long–Evans rats (Harlan Laboratories) were handled and received daily intraperitoneal vehicle (0.9% saline) injections for 4 d. On the fifth day, the rats were injected intraperitoneally with NMDA receptor antagonist 3-(2-carboxypiperazin-4-yl)propyl-1-phosphonic acid (CPP) (10 mg/kg in

Received July 8, 2010; revised Aug. 27, 2010; accepted Sept. 15, 2010.

This work was supported by National Institute of Mental Health (NIMH) Grant MH082042 to C.G., National Institute of Neurological Disorders and Stroke (NINDS) Grant NS45260 to C.G. and G.L., Office of Naval Research Multidisciplinary University Research Initiative Award N00014-10-1-0072 to G.L., NIMH Fellowship MH083396 to L.C., and NINDS fellowship NS045540 to C.R. We thank Rishi Mehta, Ignacio Rivera, and Katherine M. Wong for expert technical assistance.

Correspondence should be addressed to Christine M. Gall, Gillespie Neuroscience Research Facility, 837 Health Science Road, University of California, Irvine, Irvine, CA 92697-4291. E-mail: cmgall@uci.edu.

DOI:10.1523/JNEUROSCI.3549-10.2010

 0270-6474/10/3015097-05$15.00/0

0.9% saline) or vehicle 30 min before placement in the video-monitored USL box or being returned to home cages. Thirty minutes later, the animals were anesthetized with fluorothane and decapitated. Brains were rapidly removed, frozen in 2-methylbutane (−55°C, ~1 min), and cryostat sectioned (20 μm, coronal). Sections were cold-mounted onto slides, gradually warmed to room temperature, fixed in methanol (−20°C, 10 min), and stored at −20°C.

Immunohistochemistry. Sections to be compared were processed simultaneously for double immunofluorescence as described previously (Chen et al., 2007) using a primary antisera cocktail containing mouse anti-PSD95 (1:1000; Affinity Bioreagents, #MA1-045) and rabbit antisera to phosphorylated (p) Trk^{Y490} (1:200; Cell Signaling Technology, #9141), pTrkB^{Y515} (1:200; Abcam, #ab51187), or TrkB (1:1000; Biosource, #611641) and a secondary antisera cocktail containing Alexa594 anti-rabbit IgG and Alexa488 anti-mouse IgG (Invitrogen). Control sections were similarly processed but with individual primary antisera omitted.

Imaging and quantitative analysis. Immunolabeled sections were examined using an epifluorescence microscope (Leica DM6000) with a 63× PlanApo objective (numerical aperture 1.4) and a CCD camera (ORCA-ER, Hamamatsu). Digital image *z*-stacks (0.2 μm *z*-steps through 3 μm) were collected from sample fields (136 × 105 × 3 μm) within stratum (str.) radiatum of CA3a, CA1a, and CA1b, CA3a str. lucidum, and the dentate gyrus molecular layer (internal blade). Images were processed for restorative deconvolution (Volocity 5.0, Improvision) corrected by point-spread functions from a 3D reconstruction of TetraSpeck fluorescent microspheres (Invitrogen). In-house built software (Matlab, C, Perl) was used to perform image intensity normalization and segmentation to identify immunolabeled elements and quantify the numbers and volumes of immunoreactive puncta as described previously (Rex et al., 2009). Element counts from each of 10–15 serial sections per zone (subfield and septotemporal placement) were averaged to produce an animal mean for that region. For cross-section reconstructions, image montages were collected automatically across a preassigned contiguous grid and stitched using Leica MetaMorph Acquisition software (Molecular Devices).

Statistics. Unless otherwise stated, values presented are group means ± SEM. Significance of treatment effects was determined using two-tailed *t* tests or ANOVAs followed by Tukey's HSD *post hoc* test (SPSS Statistics, IBM). Frequency and cumulative frequency distributions represent pooled data across all animals within a group. Group frequency distribution differences were assessed using the Kolmogorov–Smirnov (K–S) *z* test followed by the more stringent one-way Kruskal–Wallis nonparametric test to account for differences between animals.

Results

Localization of phospho-Trk in rostral hippocampus

A sizable literature indicates that the hippocampus is critical for USL of novel environments (Roberts et al., 1962; Cohen, 1970; O'Keefe and Nadel, 1978). We therefore used a variant of this paradigm for the present studies. Rats were handled and acclimated to intraperitoneal vehicle injections for 4 d. On the following test day, home cage (HC) control and experimental/USL rats were transported to the test room, but only the latter were introduced into the complex environment for the 30 min test session. The two groups (HC and USL) were subdivided into subsets pretreated with vehicle or the centrally active NMDA receptor antagonist CPP, at concentrations (10 mg/kg) that block long-term potentiation (LTP) (Abraham and Mason, 1988) and long-term memory in multiple tasks (Ward et al., 1990; Mele et al., 1996), including USL (Fedulov et al., 2007; Chen et al., 2010). In agreement with previous reports (Fedulov et al., 2007; Chen et al., 2010), an analysis of motion tracking data showed that the distance traveled by vehicle-treated animals decreased steadily over the course of the unsupervised learning session ($p < 0.05$ initial 5 min vs final 5 min; Tukey's HSD). CPP did not measurably influence these time-dependent effects or the mean velocity of movement ($p > 0.05$, vehicle vs CPP groups, repeated-measures ANOVA).

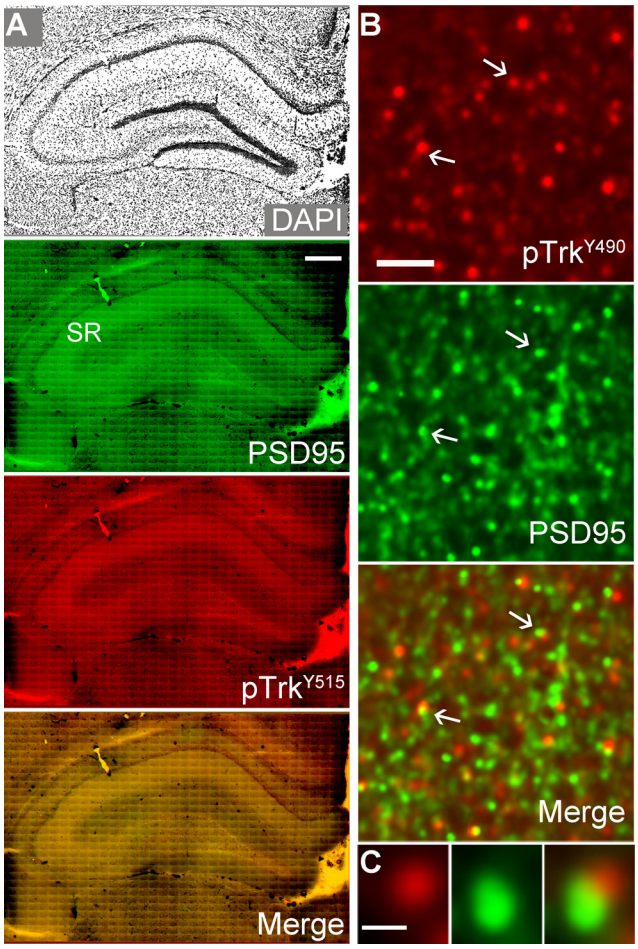

Figure 1. Phosphorylated Trk is localized to postsynaptic densities. ***A***, Montages of photomicrographs collected from dorsal hippocampus show DAPI labeling of nuclei (top; image intensities inverted), immunofluorescence labeling for PSD95 (green) and pTrkB^{Y515} (red), and a merger of PSD95 and TrkB^{Y515} immunolabeling (sr: str. radiatum; scale bar: 500 μm). The pTrkB^{Y515} and pTrk^{Y490} immunoreactivities have similar distributions in hippocampus (supplemental Fig. 1, available at www.jneurosci.org as supplemental material) (also, Chen et al., 2010). ***B***, Representative deconvolution micrographs show immunofluorescence for pTrk^{Y490} (red) and PSD95 (green) in CA3a str. radiatum. Arrows indicate double-labeled elements (yellow in "merge"). Scale bar: 10 μm. ***C***, High magnification of a single synapse double-labeled for pTrk^{Y490} (red) and PSD95 (green). Scale bar: 1 μm.

Phospho-specific antisera directed against the conserved Trk Tyr490 residue (Trk^{Y490}), which is phosphorylated with Trk activation, were used to study the effects of learning on BDNF signaling in rostral hippocampus (2.2 mm to 2.8 mm posterior to bregma) (Paxinos, 1986). Most immunostaining for pTrk was localized to small dense structures that were evenly distributed across str. radiatum of hippocampal fields CA3 and CA1 (Fig. 1*A*; supplemental Fig. 1, available at www.jneurosci.org as supplemental material). Deconvolved immunofluorescence images showed that pTrk-immunopositive (+) elements were commonly, although not ubiquitously, double-labeled with antisera to the postsynaptic density (PSD) scaffold protein PSD95 (Fig. 1*B*,*C*). As described below, only a small percentage of the PSDs were pTrk immunoreactive.

Learning-related phosphorylation of synaptic Trk varies across subfields

Blind, automated counting indicated that 3.7 ± 1.0% (mean ± SEM) of the total PSD population was immunolabeled for pTrk

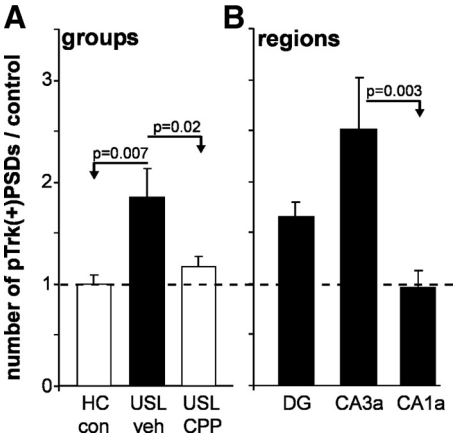

Figure 2. Learning-related increases in numbers of pTrk^{Y490}+ synapses are regionally differentiated in rostral hippocampus. The mean (± SEM) number of double-labeled synapses (pTrk(+)PSDs) in the sample field is expressed as a ratio of the HC control mean (indicated by dashed line). ***A***, Overall numbers of double-labeled synapses (cumulative across three sampling zones) were significantly greater in vehicle (veh)-treated rats that explored the complex environment for 30 min (USL veh) than in HC controls. Treatment with CPP before exploration (USL CPP) eliminated this increase (n = 12–14/group; two-tailed t tests). ***B***, Plot shows that increases in pTrk+ PSDs in the USL-veh group were not equally distributed across hippocampal subfields (ANOVA: $p = 0.003$): Values from USL-veh rats were greater than from HC controls for the dentate gyrus molecular layer (DG) and CA3a ($p < 0.01$) but not for CA1a ($p > 0.4$).

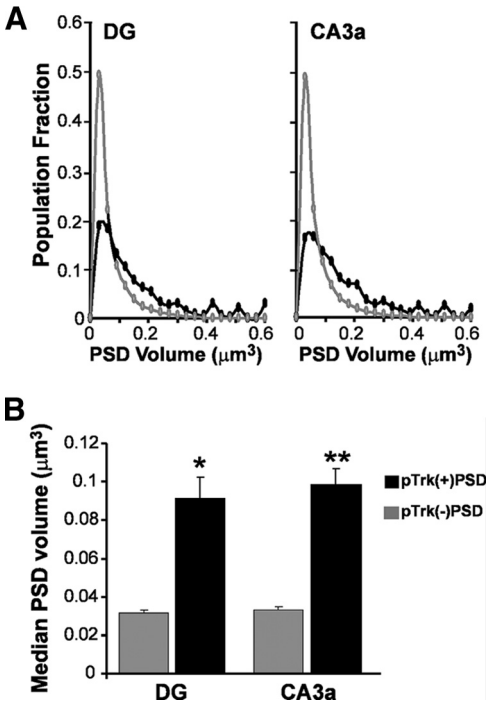

Figure 3. Synapses associated with pTrk^{Y490} are larger than neighboring, single-labeled synapses. ***A***, Volume frequency distributions for PSD95-immunoreactive elements (PSDs) that were double-labeled (black), or not double-labeled (gray) for dense pTrk^{Y490} immunoreactivity in the dentate gyrus molecular layer (DG) and CA3a str. radiatum. The pTrk+ PSD volumes were normally distributed, whereas pTrk-negative PSD volumes followed a Poisson distribution (for each region: $n > 3400$ and $n > 197{,}000$ for double- and single-labeled PSDs, respectively; $p < 0.0000001$, K–S test). ***B***, Bar graph shows the mean (±SEM) of the median volumes (per individual) of double-labeled (pTrk(+)PSD) and single-labeled (pTrk(−)PSD) PSDs for the HC and USL-veh groups ($n > 40$ sections from 4 rats each; *$p = 0.004$, **$p = 0.0004$; paired two tailed t test).

in CA3a str. radiatum of home cage control rats; values for the dentate gyrus molecular layer (DG) and field CA1a were also low (3.5 ± 0.4% and 5.6 ± 1.8%, respectively). Similar results were obtained for home cage rats injected with CPP (CA3a: 4.4 ± 1.3%; DG: 4.6 ± 1.0%; CA1a: 4.3 ± 1.0%), indicating that the NMDAR antagonist by itself had little if any effect on synaptic pTrk levels. Accordingly, we combined the results for the two home cage groups into a single control group. To facilitate comparisons of experimental effects across regions and groups, we expressed all counts from USL rats as a fraction of the mean for each region of the appropriate yoked, home cage control cohort. The experimental predictions were that (1) 30 min of unsupervised learning would increase the number of pTrk+ synapses above that found in home cage controls, and (2) this effect would be reduced by pretreatment with CPP. Automated analysis of pTrk+ PSDs confirmed both points: Mean counts across the three sampling regions were ~70% greater in USL-vehicle rats than in home cage controls ($p = 0.014$, t test, 2-tailed) or USL-CPP groups ($p = 0.04$) (Fig. 2*A*). As noted, the CPP dose used here did not affect the distance traveled or movement velocity, although it is known from past work to reduce long-term (24 h) retention of USL (Fedulov et al., 2007). Accordingly, the marked increase in double labeling found in the present USL-vehicle rats is not likely due to locomotor activity.

We next tested whether the increases in double-labeled PSDs were uniformly distributed across sampling zones in the USL-vehicle group. While values were clearly elevated above control for the DG (1.7 ± 0.3-fold; $p = 0.001$) and CA3a (2.5 ± 1.1; $p = 0.004$), those for CA1a were not detectably different from the control groups (1.0 ± 0.4) (Fig. 2*B*). The regional differences (among DG, CA3a, and CA1a) in the USL-vehicle group were highly significant ($p = 0.003$; repeated-measures ANOVA), and CA3a had more pTrk+ synapses than the DG ($p < 0.05$) or CA1a ($p < 0.01$). The numerical results for CA3a are comparable to those described previously for field CA1b (2.3 ± 0.2-fold control) (Chen et al., 2010). No differences were observed among subfields for numbers of PSDs double-labeled for total (phosphorylated and nonphosphorylated) TrkB (supplemental Fig. 2, available at www.jneurosci.org as supplemental material), confirming that the above effects were not due to regional variations in the expression of the receptor itself. These results provide the first evidence that USL-associated increases in Trk signaling occur in a regionally differentiated manner.

Phosphorylated Trk is associated with expanded PSDs in dorsal hippocampus

Certain actin signaling events found at synapses during the production of LTP in hippocampal slices (Chen et al., 2007; Lynch et al., 2008) also occur during unsupervised learning (Fedulov et al., 2007). In both cases, PSD95+ synapses double-labeled for the LTP marker pCofilin were larger than neighboring contacts. The present results provide a second label (pTrk) for testing the idea that LTP-related signaling is associated with synapse expansion *in vivo*. We therefore measured the volumes of the PSD95+ elements colocalized with dense pTrk^{Y490} immunoreactivity and compared these values with those for surrounding PSDs that were not double-labeled.

Single- and double-labeled PSD volume frequency distributions were constructed from the 1.3 million measurements collected for the DG and CA3a of USL-vehicle rats. The distributions were clearly different for pTrk^{Y490}-negative vs pTrk^{Y490}-positive PSDs in both sampling zones (Fig. 3*A*) ($p < 0.000001$ each region, K–S test). The pTrk^{Y490}-positive contacts generated a near-Gaussian distribution, while the much larger population of single-labeled synapses formed a Poisson (Fig. 3*A*). As expected

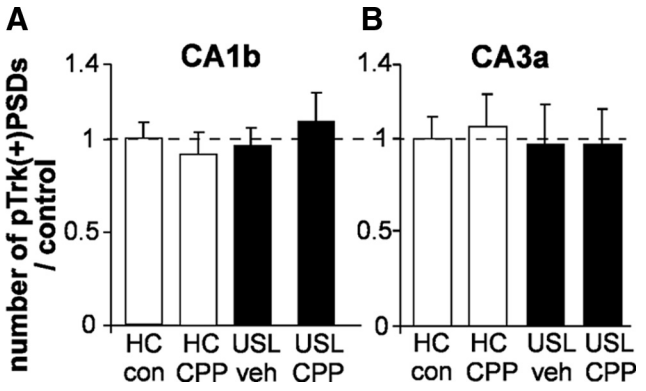

Figure 4. USL does not increase numbers of pTrk^{Y490}+ synapses in temporal hippocampus. Summary of double-labeled synapses (pTrk(+)PSDs) in CA1b (***A***) and CA3a (***B***) str. radiatum of temporal hippocampus expressed as a function of the home cage control mean (HC con). ***A***, Plot shows that 30 min of USL, with or without CPP treatment, had no effect on numbers of pTrk+ PSDs in temporal CA1b. ***B***, There were no significant differences in numbers of pTrk+ PSDs in temporal CA3a among the four groups ($p > 0.3$ for HC-CPP rats and the two USL groups vs HC controls).

from these differences, the individual animal median volumes for PSD95+ puncta were markedly different for single- versus double-labeled PSDs in each field (Fig. 3*B*) (DG: $p = 0.004$; CA3a: $p = 0.0004$; paired *t* test, two tails). These effects were also evident in cumulative volume distributions for the three hippocampal subfields in both USL-vehicle and control-vehicle animals ($p < 0.000001$ each region, two-sample K–S test; supplemental Fig. 3, available at www.jneurosci.org as supplemental material).

Given that previous work established that measures of synapse size are not affected by double labeling per se (Chen et al., 2007), the above results support the conclusion that synapses associated with LTP-related markers are significantly larger than surrounding contacts *in vivo*.

TrkB changes are absent in the temporal hippocampus

Neurobehavioral studies indicate that the rostral hippocampus is critical for spatial learning, while more temporal portions are not required for place coding in paradigms lacking an explicit reward (Moser and Moser, 1998; Bast et al., 2009; Fanselow and Dong, 2010). We therefore tested whether increases in pTrk found in rostral hippocampus (above) are equally well developed in more temporal regions. To this end, coronal sections were evaluated from the zone extending from 3 to 5 mm posterior to bregma (Paxinos, 1986).

In marked contrast to the more than twofold increases in pTrk+ PSDs obtained in rostral hippocampus (Chen et al., 2010), there was no evident effect of learning on Trk phosphorylation in field CA1b in temporal hippocampus (fold of home cage controls: HC-vehicle vs USL-vehicle: 1.0 ± 0.1 vs 1.1 ± 0.3; $n = 12$ animals/group). Indeed, the number of double-labeled synapses in CA1b was not detectably different across the two home cage (vehicle, CPP) and two USL groups (Fig. 4*A*).

Given that CA1a did not show a learning effect in rostral hippocampus, and the possibility that boundaries between CA1a and CA1b might differ across the septotemporal axis, we repeated the experiment by counting double-labeled synapses in the clearly defined temporal CA3a. We again found no evidence for a USL-induced increase in pTrk+ contacts ($p > 0.3$) (Fig. 4*B*).

Combined, the results indicate that the robust effects of USL on BDNF signaling in rostral hippocampus do not occur in more temporal regions.

Discussion

The present results indicate that a form of learning common to mammals, and prominent in humans, is associated with the activation of synaptic BDNF receptors in hippocampus and that synapses with active Trk signaling are larger than their neighbors. The increases in Trk activation were likely related to encoding, rather than to locomotor activity, because they were blocked by an amnestic dose of an NMDA receptor antagonist that does not cause changes in the distance traveled in the complex environment. The same drug treatment had no measurable influence on basal pTrk immunolabeling in home cage control rats, so its actions in the learning paradigm can be attributed to a selective suppression of behaviorally induced increases. The larger volume of pTrk+ synapses relative to surrounding contacts lacking Trk activation is novel but accords with previous evidence for an enlargement of synapses exhibiting LTP-related signaling *in vitro* and *in vivo* (Chen et al., 2007; Fedulov et al., 2007).

The learning-related increases in pTrk, while pronounced, were unexpectedly restricted in their spatial extent. With regard to subdivisions of hippocampus, increases in pTrk+ PSDs were evident in str. radiatum of CA3b and CA1b, present but less pronounced in the dentate molecular layer, and absent from apical CA1a. More striking still, the effects obtained in fields CA1b and CA3a of rostral hippocampus were absent in more temporal regions of the structure. These results provide the first evidence that USL-induced, synaptic BDNF signaling is restricted to a relatively small portion of hippocampus.

What mechanisms could account for marked regional differences in neurotrophic responses within the same forebrain structure? Recent work has shown that LTP is less robust in temporal than in dorsal hippocampus and suggests that this is due to differential distributions of mineralocorticoid receptors (Maggio and Segal, 2009). There is also evidence that the LTP threshold is higher in temporal regions, possibly because of differences in adenosine "tone" (Colgin et al., 2004). Given that the conditions needed for synaptic TrkB responses and LTP induction overlap extensively (Chen et al., 2010), these observations raise the possibility that the threshold for TrkB activation increases along the septotemporal axis of hippocampus; if so, then the same USL-elicited firing patterns that pass threshold for TrkB activation in septal fields may fail to do so more temporally.

Pertinent to the above, we recently found short trains of theta burst stimulation to be the most effective pattern for activating synaptic TrkB among a set of afferent stimulation regimens, including a high-frequency train, using the same number of electrical pulses. The mechanisms underlying the differential efficacy involved an NMDA receptor-initiated cascade targeted at BDNF receptors (Chen et al., 2010). Given these points, it is of interest that theta activity power and the incidence of spatially tuned neurons are both reduced in the temporal portion of the hippocampus relative to more rostral areas (Buzsáki, 2005). Possibly then, a relative weakness of theta activity, and the burst firing that accompanies it during behavior (Otto et al., 1991), results in a lower probability of engaging synaptic TrkB signaling in temporal hippocampus.

There have been no studies identifying optimal stimulation parameters for eliciting TrkB phosphorylation, or stable LTP, in temporal hippocampus. If regional differences do exist, then a synthetic hypothesis would be possible in which different types of learning trigger characteristic patterns of input to the hippocampus, and thereby elicit TrkB activation in portions of the structure

"tuned" to that pattern but not in areas responsive to other signals.

Functionally, the spatially restricted distribution of synaptic effects suggests that the hippocampus is economical with regard to neuronal resources used to store new information. The learning episode lasted for only 30 min, and it is conceivable that different kinds of material acquired in the complex environment over additional days of testing would engage CA1a or regions further down the septotemporal axis. The hippocampus could, for example, use space to segregate the types of data acquired through USL (e.g., spatial cues on day 1 vs objects on day 2) or to maintain a record of when particular memories were encoded. Along this line, there is evidence that ventral hippocampus is involved in encoding the sequence of odor cue presentation (Hunsaker et al., 2008; Kesner et al., 2010). More generally, the striking absence of Trk phosphorylation in temporal areas is consonant with past arguments that different portions of hippocampus are involved in different types of memory. Results from lesion and chronic recording experiments suggest that the rostral, but not temporal, hippocampus is required for acquisition of spatial information in the absence of explicit reward (Morris et al., 1982; Packard and McGaugh, 1996), while temporal hippocampus plays a critical role in reward-based learning (Bast et al., 2009), something that might be expected given its close relationship to the amygdala (Monfils et al., 2007).

The present findings also raise a series of novel questions about the function of learning-related neurotrophic signaling at synapses. Increases in the number of synapses labeled for activated Trk were large relative to the low values found in home cage rats but nonetheless involved a very small percentage of the total synaptic population. Is this sufficient to trigger genomic responses in the neurons on which the Trk response occurred? Answering this experimentally tractable question would be a significant step in evaluating the argument that learning plays a critical role in maintaining the viability of neurons.

References

Abraham WC, Mason SE (1988) Effects of the NMDA receptor/channel antagonists CPP and MK801 on hippocampal field potentials and long-term potentiation in anesthetized rats. Brain Res 462:40–46.

Bast T, Wilson IA, Witter MP, Morris RG (2009) From rapid place learning to behavioral performance: a key role for the intermediate hippocampus. PLoS Biol 7:e1000089.

Buzsáki G (2005) Theta rhythm of navigation: link between path integration and landmark navigation, episodic and semantic memory. Hippocampus 15:827–840.

Castrén E, Berninger B, Leingärtner A, Lindholm D (1998) Regulation of brain-derived neurotrophic factor mRNA levels in hippocampus by neuronal activity. Prog Brain Res 117:57–64.

Chao MV (2003) Neurotrophins and their receptors: a convergence point for many signalling pathways. Nat Rev Neurosci 4:299–309.

Chen LY, Rex CS, Casale MS, Gall CM, Lynch G (2007) Changes in synaptic morphology accompany actin signaling during LTP. J Neurosci 27:5363–5372.

Chen LY, Rex CS, Sanaiha Y, Lynch G, Gall CM (2010) Learning induces neurotrophin signaling at hippocampal synapses. Proc Natl Acad Sci U S A 107:7030–7035.

Cohen JS (1970) Exploration in the hippocampal-ablated albino rat. J Comp Physiol Psychol 73:261–268.

Colgin LL, Kubota D, Jia Y, Rex CS, Lynch G (2004) Long-term potentiation is impaired in rat hippocampal slices that produce spontaneous sharp waves. J Physiol 558:953–961.

Fanselow MS, Dong HW (2010) Are the dorsal and ventral hippocampus functionally distinct structures? Neuron 65:7–19.

Fedulov V, Rex CS, Simmons DA, Palmer L, Gall CM, Lynch G (2007) Evidence that long-term potentiation occurs within individual hippocampal synapses during learning. J Neurosci 27:8031–8039.

Greenberg ME, Xu B, Lu B, Hempstead BL (2009) New insights in the biology of BDNF synthesis and release: implications in CNS function. J Neurosci 29:12764–12767.

Huang YZ, McNamara JO (2010) Mutual regulation of Src family kinases and the neurotrophin receptor TrkB. J Biol Chem 285:8207–8217.

Hunsaker MR, Fieldsted PM, Rosenberg JS, Kesner RP (2008) Dissociating the roles of dorsal and ventral CA1 for the temporal processing of spatial locations, visual objects, and odors. Behav Neurosci 122:643–650.

Isackson PJ, Huntsman MM, Murray KD, Gall CM (1991) BDNF mRNA expression is increased in adult rat forebrain after limbic seizures: temporal patterns of induction distinct from NGF. Neuron 6:937–948.

Kalb R (2005) The protean actions of neurotrophins and their receptors on the life and death of neurons. Trends Neurosci 28:5–11.

Kesner RP, Hunsaker MR, Ziegler W (2010) The role of the dorsal CA1 and ventral CA1 in memory for the temporal order of a sequence of odors. Neurobiol Learn Mem 93:111–116.

Lynch G, Rex CS, Chen LY, Gall CM (2008) The substrates of memory: defects, treatments, and enhancement. Eur J Pharmacol 585:2–13.

Maggio N, Segal M (2009) Differential corticosteroid modulation of inhibitory synaptic currents in the dorsal and ventral hippocampus. J Neurosci 29:2857–2866.

Mele A, Castellano C, Felici A, Cabib S, Caccia S, Oliverio A (1996) Dopamine-N-methyl-D-aspartate interactions in the modulation of locomotor activity and memory consolidation in mice. Eur J Pharmacol 308:1–12.

Minichiello L (2009) TrkB signalling pathways in LTP and learning. Nat Rev Neurosci 10:850–860.

Monfils MH, Cowansage KK, LeDoux JE (2007) Brain-derived neurotrophic factor: linking fear learning to memory consolidation. Mol Pharmacol 72:235–237.

Morris RG, Garrud P, Rawlins JN, O'Keefe J (1982) Place navigation impaired in rats with hippocampal lesions. Nature 297:681–683.

Moser MB, Moser EI (1998) Functional differentiation in the hippocampus. Hippocampus 8:608–619.

O'Keefe J, Nadel L (1978) The hippocampus as a cognitive map. Oxford: Oxford UP.

Otto T, Eichenbaum H, Wiener SI, Wible CG (1991) Learning-related patterns of CA1 spike trains parallel stimulation parameters optimal for inducing hippocampal long-term potentiation. Hippocampus 1:181–192.

Packard MG, McGaugh JL (1996) Inactivation of hippocampus or caudate nucleus with lidocaine differentially affects expression of place and response learning. Neurobiol Learn Mem 65:65–72.

Paxinos G (1986) The rat brain in stereotaxic coordinates, Ed 2. San Diego: Academic.

Rex CS, Chen LY, Sharma A, Liu J, Babayan AH, Gall CM, Lynch G (2009) Different Rho GTPase-dependent signaling pathways initiate sequential steps in the consolidation of long-term potentiation. J Cell Biol 186:85–97.

Roberts WW, Dember WN, Brodwick M (1962) Alternation and exploration in rats with hippocampal lesions. J Comp Physiol Psychol 55:695–700.

Schacter D (1982) Stranger behind the engram: theories of memory and the psychology of science. Hillsdale, NJ: Erlbaum.

Tapia-Arancibia L, Aliaga E, Silhol M, Arancibia S (2008) New insights into brain BDNF function in normal aging and Alzheimer disease. Brain Res Rev 59:201–220.

Valenzuela MJ, Breakspear M, Sachdev P (2007) Complex mental activity and the aging brain: molecular, cellular and cortical network mechanisms. Brain Res Rev 56:198–213.

Ward L, Mason SE, Abraham WC (1990) Effects of the NMDA antagonists CPP and MK-801 on radial arm maze performance in rats. Pharmacol Biochem Behav 35:785–790.